Water-Gas Imbibition Relative Permeability: Literature Review, Direct versus Indirect Methods and Experimental Recommendations

Fabrice Pairoys[1], *Cyril* Caubit[1]

[1]TOTALENERGIES CSTJF, Pau, France

Abstract. When an active aquifer encroaches into a gas bearing reservoir or when an oil rim sweeps gas during late depletion of the gas cap, gas displacement by liquid is important for estimating the gas recovery. In the water displacing gas condition, the viscosity ratio is extremely favorable, resulting in a sharp waterfront in the reservoir matrix: it results that changing the relative permeability Kr shape has negligible effect, while endpoints water relative permeability Krw Max and residual gas saturation Sgr are much more important to understand gas flow performance for estimation of gas recovery with active aquifer or productivity decline after water breakthrough. Three main methods are used to determine water/gas relative permeability curves: imbibition unsteady-state, imbibition steady-state or indirect approaches such as co-current spontaneous imbibition if transient data are available. One of the other popular indirect methods is called Brooks-Corey approach: by measuring the drainage Pc curve using centrifuge or porous plate methods, it is possible to calculate a pore size distribution index λ. This coefficient is used in a Brooks-Corey model to determine the drainage Kr curve. It is also required to measure and determine the relationship between the residual gas saturation Sgr and the initial gas saturation Sgi relationship. Finally, it is accepted that there is no hysteresis on the water relative permeability Krw curve, as water is always the wetting phase in the gas/water couple. As non-wetting phase, gas exhibits strong hysteresis between drainage and imbibition curves: it is therefore necessary to apply a correction on the drainage Krg curve to build the imbibition one using correcting models. The aim of this paper is to compare gas/water relative permeability of clastic rocks using direct waterflooding information and indirect approach using Brooks-Corey model. It is shown that using the indirect approach leads to results like those experimentally obtained. Also, additional numerical simulations are proposed to discuss the relevance of measuring the entire water-gas imbibition relative permeability curve using the steady-state approach.

1 Introduction

Trapping mechanisms at pore scale of non-wetting fluids such as gas (versus liquids) have been mainly investigated through observations using glass micromodels or transparent glass bead systems. Micro-CT recently started 3D imaging of trapped gas in rocks to better understand this trapping phenomenon. Both techniques have shown that gas phase is trapped as discontinuous phase at the middle of the large pores while water occupies smaller pores as shown by [1].

Different types of displacement mechanisms in imbibition cycle have been put in evidence on glass micromodels by [2]: it is shown that, in liquid-wet domain, the imbibition is mainly dependent on pore size distribution and contact angle. Later, [3], [4] and [5] showed that:

- The ratio between pore throat and pore diameters (aspect ratio) matters, with more trapping at larger aspect ratio
-   The number of pore throats connected to a given pore is also very important on trapping, with large coordination numbers tending to lead to less trapping
- An increase in contact angle suppresses snap-off, leading to less trapping

If these results have been observed on glass micromodels and pore network models, micro-CT should confirm the above-mentioned trends. Today, the resolution of micro-CT systems limits these investigations to fair to very good quality rocks.

At the macroscopic scale, in most cases, the displacement of gas by liquid occurs at favorable to extremely favorable viscosity ratios. During laboratory experiments, there is no or negligible variation of gas saturation after the water breakthrough. In the field, flood is almost piston-like in the reservoir matrix, with no mobile gas behind the waterfront. It is finally concluded that attention is devoted to Sgr and maximum Krw value at Sgr rather than the shape of the Kr curve. Nevertheless, imbibition relative permeability bounding curve, measured or derived, is still required for reservoir numerical simulations.

In this paper, we made a literature review on the methods to estimate the residual gas saturation, looking at the parameters that can affect Sgr, providing tips for the waterflooding tests. Also, the indirect Brooks-Corey approach, coupled with the Land's hysteresis model, was tested and compared to the experimental data results. It confirmed the findings and conclusions from [6].

2 Background

2.1 Experimental Methods to estimate Sgr

Several gas/water imbibition experimental methods can be used to determine Sgr:

---

* Corresponding author: fabrice.pairoys@totalenergies.com

- Porous plate method: after a primary drainage of water displaced by humidified nitrogen at highest capillary pressure, Pc is then gradually decreased in a stepwise manner allowing controlled imbibition of gas-saturated water. Residual gas is obtained by material balance when the capillary pressure Pc=0. This test is time-consuming, especially on low permeability rocks. On very low permeability samples, mercury imbibition can be attempted to obtain trapped non-wetting phase saturation, but it is not recommended.

- Unsteady-state method; it is a forced displacement of gas by water at constant low rate Qw or low differential pressure dP. Residual gas saturation Sgr is obtained at the end of the flood when the gas production ceases (generally right after the water breakthrough). In situ saturation monitoring is recommended: it generally confirms the sharp front with no variation of the gas saturation behind the front

- Steady-state method: it is a co-injection of gas and water, but it is not the best appropriate approach to determine Sgr, except maybe on heterogeneous rocks and gas/condensate studies. It can be used to obtain the full Kr curve

- Spontaneous imbibition by water or capillary rise method: it is the most popular technique to determine Sgr. The spontaneous imbibition test requires a strongly wetting liquid to achieve a non-wetting residual saturation. Two configurations exist: co-current and counter-current displacements, respectively with the liquid touching the bottom of the rock (capillary rise test) and with the rock fully immersed in the liquid

Based on the past literature, there is no ideal technique and decision of choosing such or such method: it is case dependent. [7] and [8] reported very similar trapped gas saturations using steady-state, unsteady-state and spontaneous imbibition. More recently, some studies from [9] put in evidence some significant differences on Sgr computed from the different methods. Based on the above observations, it is recommended to make a combination of techniques during a study. Important to note that large uncertainty in results is anticipated for very tight gas reservoirs with porosity ϕ below 5% and permeability K below 0.01 mD. In this specific case we won't develop in this work, non-standard approach such as evaporation method may be tested.

2.2 Various Potential Effects on Sgr (Literature review and in house experience)

Regarding the types of liquid, [10] showed that same trapped gas saturation is found using different imbibing fluids, provided the liquids strongly wet the rock.

For the forced displacements, it is recommended to perform the liquid injection at low rate despite most of the past studies show no Sgr dependency on displacement rate ([7], [8], [11]: only [9] showed significant differences in Sgrw values between porous plate method and unsteady-state coreflooding tests.

Fluid pressure or temperature do not affect residual gas saturation ([11], [12]), [13], [14]).

Regarding the effect of wettability, it is always assumed that gas is the non-wetting phase and liquid the wetting phase. However, it was early observed by [7] that some cores could imbibe oil but not water. It was confirmed by in house tests, showing that water is not always strongly wetting the rock in respect to gas. When water is not imbibing the rock, other fluids can be tested, such as toluene or refined oil: in house experience and literature have showed that these liquids are sometimes more wetting the rock than water ([15], [16]). When poor water wetness is observed, it can either result from true original reservoir wettability or from core contamination.

Effect of Sgi on Sgr:

Residual gas saturation Sgr strongly depends on initial gas saturation, both on sandstones ([7], [10], [14], [17]) and on carbonates ([18]). Several formulas can be used to capture this effect: the most used is the Land's formula ([17]):

$$\frac{1}{S_{gr}^*} - \frac{1}{S_{gi}^*} = C = \frac{1}{S_{gr(Swi)}} - \frac{1}{1-S_{wi}} \qquad \text{Eq 1}$$

$$S_{gi}^* = \frac{S_{gi}}{1-S_{wi}} \text{ and } S_{gr}^* = \frac{S_{gr}}{1-S_{wi}} \qquad \text{Eq 2}$$

Other ones like [18] or [19] are available.

[21] measured the residual gas saturation Sgr as function of initial gas saturation Sgi on 60 sandstone samples. Their porosity and permeability ranged from 0.06 to 0.25 and from 0.1 to 2000 mD. Sgrm values ranged from 0.04 to 0.65. It was confirmed that the piecewise linear relationship from [19] is the best relationship to describe Sgr-Sgi curves. None of the hyperbolic laws can correctly describe the observed experimental behavior. The relationship from [20] gave the poorest estimates of Sgr as a function of Sgi.

The existence of Sgr plateau as Sgi decreases is linked to the absence of gas trapping inside micropores. Assuming pores are drained in order of size while Sgi increases, the lowest Sg value of the piecewise linear and horizontal relationship between residual and initial gas saturation may be defined as the limit between drained pores that trap gas and pores too small to trap gas. It indirectly confirms that there is no gas trapping in micropores.

Despite it was observed that model from [19] best captures experimental relationships between Sgr and Sgi, the industry and particularly numerical codes continue using Land's model.

Effect of rock properties, Sgr versus porosity with or without clays:

It has been observed large Sgr variations in a given field with decreasing Sgr trend as porosity increases ([14]) but several in house and external studies have shown more complex trends ([9]). [22] has collected data results from the literature showing wide dispersion of the maximum residual gas saturation Sgrm/porosity cross plot:
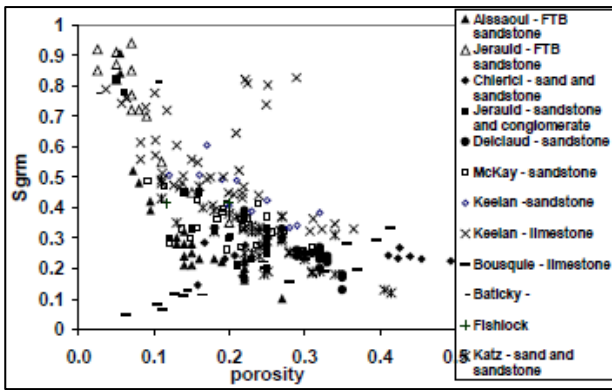
Fig. 1. Literature review 1 of maximum trapped gas saturation versus porosity, in absence of irreducible water saturation

Despite some studies concluded that Sgr increases as porosity decreases, Figure 1 shows the difficulty that encountered [13] to find, in vain, a general correlation between porosity (permeability and Sgi too) and Sgr. The largest investigation was performed by [22] and [23] with more than 300 Sgr measurements on sandstones:
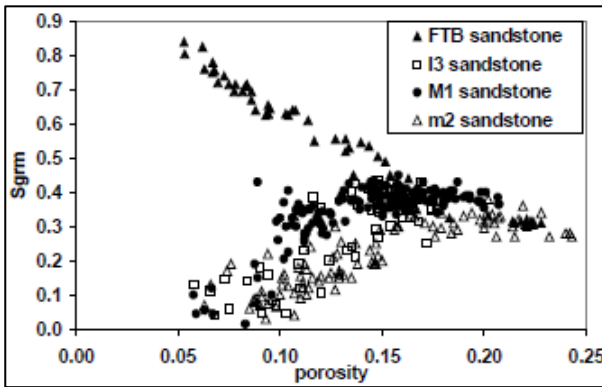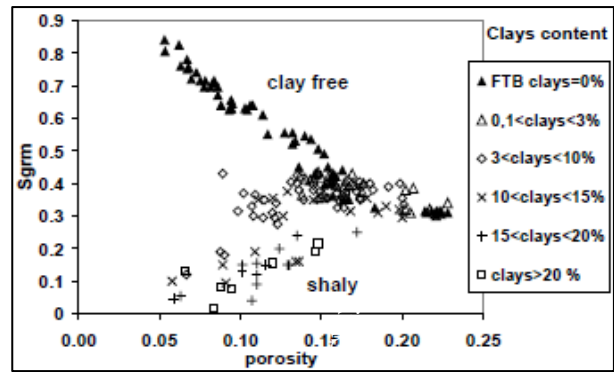

Fig. 2. Literature review 2 of maximum trapped gas saturation versus porosity in absence of irreducible water saturation

For porosity values below 15%, Figure 2 shows that Sgrm decreases for I3, M1, M2 sandstones and increases for FTB (Fontainebleau outcrops) as porosity decreases. Above 15% of porosity, the data results from all reservoirs converge, with Sgrm values varying from 25% to 35%.

The difference between the Fontainebleau sandstone and the other ones was explained by the presence of micro-porosity or clays, the Fontainebleau sandstone being mesoporous and clay-free.

Later, [24] provided the following plot of Sgrm versus porosity, adding the clay %. It shows that greater microporosity in the clay mineral assemblage enhances water imbibition and limits gas trapping.

Fig. 3. Literature review 3 of maximum trapped gas saturation versus porosity with clay %, in absence of irreducible water saturation

The observations show that assessing the variability of Sgr within a reservoir and finding clues to explain it from a sedimentological point of view are key objectives.

Based on the literature review, it is obvious that laboratory work is required to guess a trapped gas saturation. Any estimation should be given ±10 s.u. at minimum, with larger uncertainty when dealing with carbonate rocks and sandstone rocks with less than 15 p.u. porosity.

2.3 Waterflood tips:

In water displacing gas tests, most of the studies show no additional gas production post breakthrough, whatever the displacement rate as expected from a liquid-wet system. During laboratory waterflood, 1 to 2 PVs injected are enough. Moreover, as the viscosity ratio is extremely favorable, resulting in a very sharp waterfront in conventional matrix, the endpoints Sgr and Krw at Sgr are more important than the Kr shape by itself.

Some cautions are required when performing waterflood, such as equilibrating the phases to avoid any mass transfer, avoiding compressing gas in the pore network during the test. Coreflooding tests can be performed with a low solubility gas such as nitrogen, at ambient temperature and ambient or reduced pore pressure.

2.4 Deriving water/gas imbibition Kr curves from Sgr/Sgi experiments:

In strongly water wetting conditions, it is stated that the shape of the imbibition relative permeability is not important while the Sgr/Sgi relationship and Krw Max value are. Nevertheless, imbibition Kr curves are still needed as input in reservoir simulations.

They are few developed methods to obtain this Kr curve in water-wet conditions. The approach proposed by [17] is generally used when drainage gas/water Kr and Sgr/Sgi relationship are available. It assumes that:

- The water wetting phase does not exhibit any hysteresis, meaning that drainage and imbibition Krw overlay

- The gas non-wetting phase exhibits a strong hysteresis between drainage and imbibition, but imbibition Krg can be derived from drainage Krg

- The gas non-wetting phase can be treated as two separate saturations, one trapped that does not contribute to the flow, another one mobile used to calculate Krg(Sg)

2.5 Calculation Krg(Sg):

1- Imbibition starts from the maximum gas saturation post drainage

2- Sgr is derived from the experimental Sgr/Sgi relationship using Land's formula (Equation 1 and Equation 2)

3- Mobile non-wetting phase saturations S_{gF}^* are calculated for various gas saturations using the following equation:

$$S_{gF}^* = \frac{1}{2}\left(S_g^* - S_{gr}^* + \sqrt{\left(S_g^* - S_{gr}^*\right)^2 + \frac{4}{C}\left(S_g^* - S_{gr}^*\right)}\right) \quad \text{Eq 3}$$

Where Sg* is the effective total gas saturation, including trapped gas.

4- Imbibition relative permeability to gas is then calculated using:

$$K_{rg} = S_{gF}^{*2}\left(1 - \left(1 - S_{gF}^*\right)^{\varepsilon-2}\right) \quad \text{Eq 4}$$

Where the exponent ε corresponds to the drainage exponent of the wetting phase Brooks-Corey exponent detailed later ($K_{rw} = S_w^{*\varepsilon} = S_w^{*\frac{(2+3\lambda)}{\lambda}}$).

The above method implies that drainage relative permeability curve has been measured, which is, unfortunately, not always the case. Nevertheless, if primary drainage capillary pressure has been measured, drainage relative permeability can be inferred from capillary pressure.

2.6 Deriving water/gas imbibition Kr curves from water/gas drainage capillary pressure:

Assuming that the rock is strongly wetted by the liquid in the gas/liquid system, the effect of different wettability on relative permeability curves is nil. Therefore, several methods of estimation can be used to estimate gas/liquid Kr, such as [25], [26], [27], [28]. In this study, the Brooks-Corey approach ([28]) is used to determine the drainage relative permeability from the drainage capillary pressure.

The tested procedure is made several steps:

1- Obtaining drainage capillary pressure either from MICP, centrifuge or porous plate tests. It first allows to determine the various rock types and saturation function per rock type. Capillary pressure averaging is necessary to provide one single Pc curve, using Leverett J-function for instance ([29])

2- For each rock type, plot of Pc versus saturation on a log-log scale and fit the curve using a Brooks-Corey equation:

$$P_c = P_{ce}(S_w^*)^{\frac{-1}{\lambda}} \quad \text{Eq 5}$$

Where Pce is the entry capillary pressure, Sw* the reduced water saturation and λ the pore size distribution index

3- Build the drainage Brooks-Corey relative permeability curves using the above λ fitting parameter and the below equations:

$$K_{rw} = S_w^{*\frac{(2+3\lambda)}{\lambda}} \quad \text{Eq 6}$$

$$K_{rg} = (1 - S_w^*)^2[1 - (S_w^*)^{\frac{(2+\lambda)}{\lambda}}] \quad \text{Eq 7}$$

4- The resulting Brooks-Corey Krg curve must be fitted with a simple Corey function to determine the water Corey exponent nw for Krw, the water Corey exponent nw is directly calculated $n_w = \frac{2+3\lambda}{\lambda}$: the curve is now following a Corey model

5- The indirect calculated drainage Corey coefficients can be compared to the cloud of Corey coefficients from drainage Kr experimental results stored in our database

6- In parallel, plot the Sgr-Sgi relationship: in our example, the Land's method was tested, obtaining a Land's coefficient for each rock type

7- Using the drainage Krg, the Krg correction is performed to calculate Krg imbibition using Equation 4 (Krg=f[SgF*]), imbibition Krw being similar to the drainage one, ranging from Sgi to Sgr

3 Experimental Program

We present in this paper an example taken from a real gas field, with an active aquifer encroaching into the reservoir. The reservoir rock is a sandstone with low to medium clay content. Only data results from the best rock type RT1, containing no clay, are presented as example.

To validate the indirect Brooks-Corey method for inferring the imbibition relative permeability curve for a specific rock type, the experimental program consisted in:

- Measuring nitrogen/brine primary drainage porous plate capillary pressure with measurement of the maximum gas permeability KgMax at Swi

- Low imbibition waterflooding rate tests to establish Sgr/Sgi relationship with measurement of the maximum brine permeability KwMax at Sgr

- Final Dean-Stark quality check

The experimental program was performed at 3145 psi of net confining pressure and ambient temperature. To avoid gas compression, the design of the waterflooding test was done such a way the differential pressure was less than 2% of the 10 bars fluid pressure. Nitrogen and brine of 130 kppm NaCl equivalent salinity were equilibrated at the test pressure to avoid any mass transfer.

4 Experimental Results

Table 1 represents all data results collected during the program.

Table 1. RT1 core analysis properties

| Id	φ (%.)	Kkl (m D)	Swi (%)	Kg (Swi) (mD)	Sgr (%)	Kw (Sgr) (mD)	Krw (Sgr)
1	23.0	238	14.6	202	20.6	22,8	0,113
2	22.4	263	18.9	204	19.3	29,9	0,146
3	23.4	413	15.0	323	19.8	34,9	0,108
4	22.9	491	13.3	388	21.6	43,3	0,112
5	23.7	143	16.7	128	19.9	23,5	0,184
6	23.0	602	12.1	474	19.4	110	0,233
7	23.7	466	17.7	418	20.8	113	0,272

Important to note that the rock has no complex pore structure and negligible clay content.

For the rock type RT1, an averaged capillary pressure curve was obtained using the J-Leverett approach. Figure 4 represents the J-function versus water saturation Sw on a log-log plot with two "framing/bounding" functions, pessimistic and optimistic respectively:
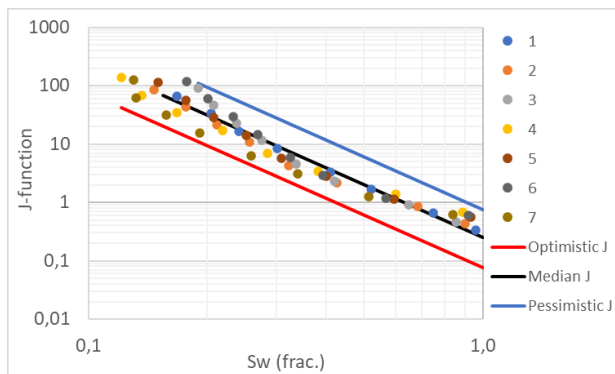
**Fig. 4.** Median J-function versus Sw with envelope

A power law type function $J=aSw^{-b}$ is used to fit the J-data points and to frame the data point cloud. In addition to the mean function plot, a pessimistic and optimistic cases were positioned to frame the J-data points. This approach results in finding associated Pc envelope in addition to the averaged Pc curve (Figure 5).
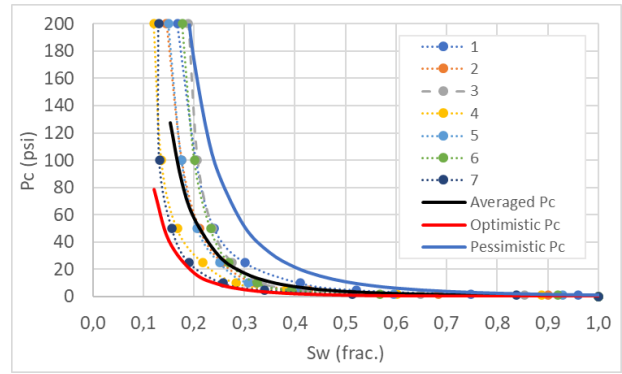
Fig. 5. Average capillary pressure Pc curve (in black) with its envelope (optimistic Pc in red, pessimistic Pc in blue)

Note that the transformation from the mean J-function to the averaged capillary pressure Pc was obtained using arithmetic average of the porosity and permeability. The Pc envelope helps the reservoir engineer to understand the uncertainty on the measured Pc and adjust its saturation's law for static reservoir modeling with observed logging information if needed.

Then, by plotting the log-log plot Pc versus effective water saturation Sw* and by using a power regression $Y=aX^b$, the respective values of entry pressure Pce (Pce=a) and pore size distribution index λ (λ=-1/b) from Equation 5 can be determined. Note that low Sw values may be discarded to obtain an acceptable correlation coefficient R^2.
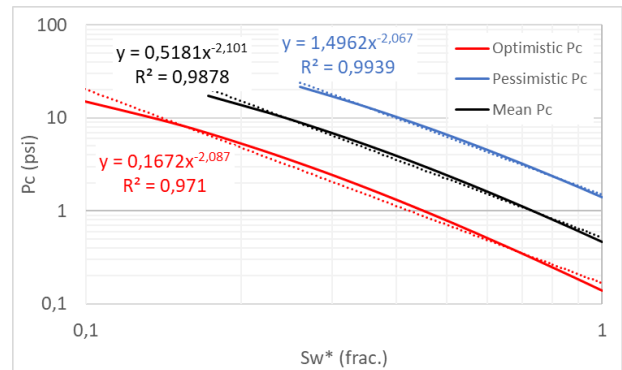
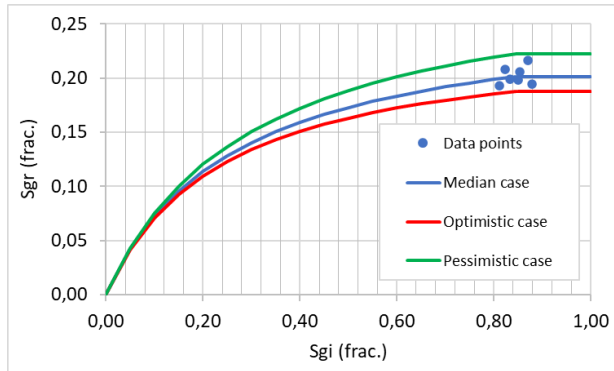
Fig. 6. Log-log plot of averaged capillary pressure Pc

The Brooks-Corey parameters can be computed from the regressions, for the averaged Pc and its envelope.

Table 2. Brooks-Corey parameters for Pc

	Optimistic Pc	Pessimistic Pc	Averaged Pc
Pce (psi)	0.17	1.50	0,52
λ	0.479	0.483	0,476
Swi (%.)	12.1	18.9	15.4

The obtained low λ values result from the good grain sorting and size, high permeability/porosity of this sandstone reservoir rock type. λ values from Table 2 are then substituted in Equations 6 and 7 to build the Kr curves. It is shown that the three λ values obtained from low case, high case and mean case are very close together. The resulting Kr curves have same curvature. The only difference is the value of Swi, according to the case.

The Sgr versus Sgi plot is then built to determine the C Land parameter that will be later used in the model.

Fig. 7. Log-log plot of averaged capillary pressure Pc

The uncertainty on Sgr values may be captured by bounding the data points cloud. For RT1, the Sgr value may vary from 18.8% to 22.3% (Figure 7). The equivalent and median C parameter was found to be equal to 3.2.

The following step shows only the median case. Using Equations 3 and 4, with the C and λ parameters determined earlier (respectively C=3.2 and λ=0.476), the imbibition Krg is then calculated. The Sgr value was taken as the average of the seven measured Sgr from Table 1. Also, the Krw Max values measured at the end of the respective waterflooding tests are plotted in Figure 8.
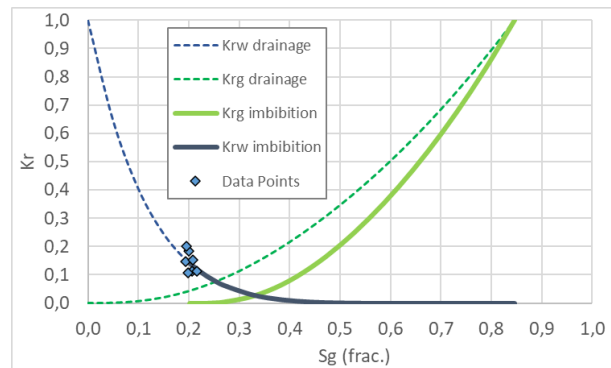
Fig. 8. Imbibition relative permeability curves from the median Pc curve and measured Krw Max at Sgr

As explained earlier, the shape of Kr curves and respective equivalent imbibition Corey exponents (Nw=7.2 and Ng=2.1) are not of high importance, only Krw Max and Sgi/Sgr relationship are. In Figure 8, it is observed that the indirect Brooks-Corey method falls in the cloud of Krw Max experimental data points. In our example, the indirect Brooks-Corey Krw Max value was

equal to 0.142 while the averaged Krw Max values measured on the seven samples was 0.145.

For the indirect Sgr value, all can understand that it must match because the value is calculated from the average of the individual and experimental Sgr values.

Note that, in our example, the nitrogen Corey exponents for drainage and imbibition modes were found to be equal, though there is a hysteresis on the Krg.

At the end of the imbibition cycle, the water saturations measured by material balance on the seven samples during the waterflooding tests are compared with the saturation measured by Dean-Stark.
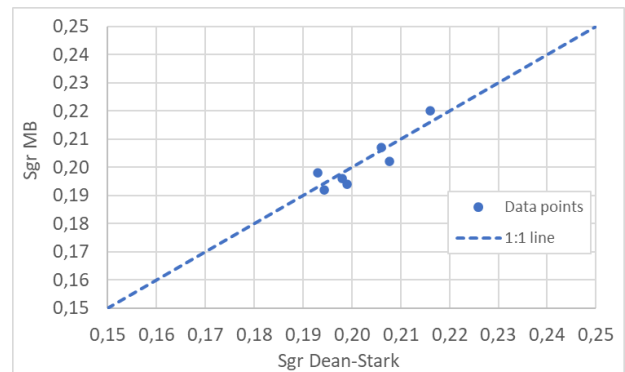
Fig. 9. Comparison between Dean-Stark Sgr and Sgr determined by material balance (Sgr MB)

Both methods lead to close Sgr values (+/- 1% S.U. max.), validating the measured production by material balance during the waterfloods.

5 Discussion

In gas-liquid imbibition cycle, it is often attempted to measure the relative permeability curve using steady-state approach. It consists in co-injecting water and gas at a total constant flowrate but varying ratios, increasing the water fractional flow.

In the case of water-gas test, where the viscosity ratio is extremely favorable and where the water is strongly wetting, we can question the relevance of performing this kind of experiment. As a matter of fact, the imbibition water-gas relative permeability curves are defined on a small range of saturation. This is because it requires extremely low water ratio to obtain data points at low water saturation. Due the experimental limitations, it may be impossible for the laboratories to design and perform such test. This statement can be proven by using numerical simulations.

CYDAR 1D numerical simulations were performed to design a steady-state relative permeability test. In our example, we used the same parameters than those presented earlier on RT1 (rock geometry and properties, fluid properties, Brooks-Corey Kr parameters, initial and final conditions).

Table 3. Simulation parameters

Rock		
L	6,60	cm
D	3,81	cm
ϕ	23,2	%
Kkl	388	mD
Fluids		
μw	1,38	cP
μg	0,017	cP
ρw	1,1	g/cc
ρo	0,001	g/cc
Kr parameters		
Nw	7,2	
Ng	2,1	
Sgi	84,6	%
Sgr	20,2	%
Krg Max	1	
Krw Max	0,142	

Note that:

- The rock properties come from the average of core plug dimensions, porosity and Klinkenberg permeability

- The fluid properties were measured for the brine, calculated for the nitrogen

- The Kr parameters come from the experimental program and Brooks-Corey Kr coefficients discussed above

A first design was tested, with no imbibition capillary pressure (Pc=0), a total constant flow rate of 100cc/h with 8 ratio and an additional bump rate at 450cc/h.

Table 4. Design for simulation

| Time (day)	Qw (cc/h)	Qg (cc/h)
25	0,01	99,99
2	0,1	99,9
2	1	99
2	10	90
2	50	50
2	80	20
2	100	0
2	450	0

The minimum flow rate for a high precision pump is around 0,01 cc/h. This rate value corresponds to the first fractional water rate applied in the simulation.
Even on the large permeability sample, the first ratio requires 25 days before obtaining equilibrium but:

- More than 50% of the produced gas is produced during this first ratio
- The dP stabilization is attained at 5 mbar, which may be readable with the resolution of the dP transducers but the confidence in the measurement is poor (high uncertainty)
- The transient saturation profiles simulated are vertical, showing no additional production after breakthrough
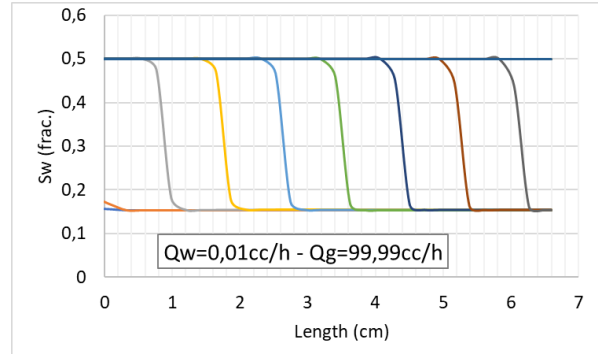
Fig. 10. Saturation profiles during the first ratio (Qt=100 cc/h)

The simulated data results with the above experimental design are presented in Figure 11.
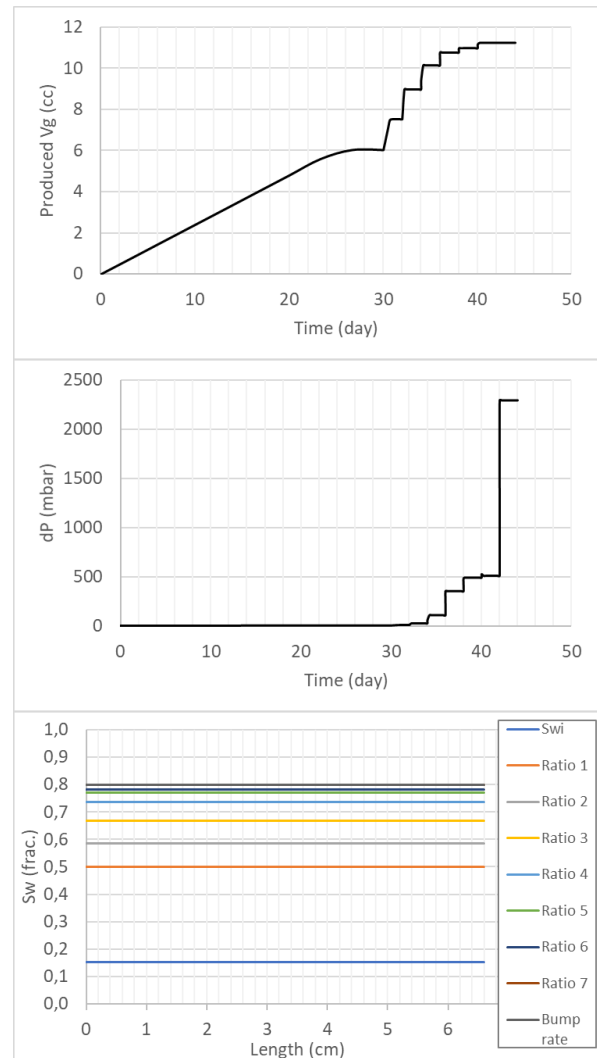
Fig. 11. Gas production, dP signal and saturation profiles at equilibrium

The simulated results presented in Figure 11 show that it is extremely difficult to measure the imbibition water-gas relative permeability. Even at the lowest water rate, the first ratio leads to more than 50% of the gas production. It is impossible to get Kr data points between Swi (=15.4%) and Sw=50%.

It is also extremely difficult to ensure good dP reading before the third ratio because of dP values at equilibrium below 30 mbars, resulting in high kr data points uncertainty too.

The Kr data points can only be defined in a reduced water saturation range 0.585<Sw<0.798, equivalent to 0.415<Sg<Sgr=0.202.

3 additional simulations were run to observe the impact of capillary pressure, considering 3 different cases:

- Case 1 is considered as an extreme case with a strongly water-wet rock, using the positive primary drainage curve. In this case, the corresponding Amott water index Iw is equal to 1

- Case 2 is a median case, less water-wet, using a log(beta) function to build a curve with a positive and negative parts. The choice was to impose a value of Sw(Pc=0) equal to 0.5. It results in Iw close to 0.5

- Case 3 is another extreme case with a significant and non-realistic negative Pc (chosen for the sensitivity study), considering the rock is not water-wet. The Sw(Pc=0) value is then equal to Swi, with no spontaneous imbibition of water. The resulting Iw is nil.

For relative permeability, same parameters than those from Table 3 were taken. Obviously, there is a problem of consistency between Kr parameters and Pc parameters for case 3 mainly (water-wet Kr vs non-water-wet Pc), but it helps in understanding the impact of Pc on the simulations thus on the steady-state experimental design.

The averaged primary drainage curve was taken to build the case 1, rescaled in the imbibition cycle saturation range. As explained previously, it is an extreme case.

A log(beta) function was used to build case 2 and case 3. It is a 3 input-parameter function [Po, β, Sw(Pc=0)] as shown in Equation 8:

$$Pc = c.Po.\ln\left(\frac{\left(1-S_w^{*\beta}\right)}{S_w^{*\beta}}\right) - b \qquad \text{Eq 8}$$

With Po a pressure coefficient to control the magnitude of the Pc curve, Sw* the reduced/normalized water saturation, β coefficient to control the asymmetry of the function, b, a function dependent on the water saturation at Pc=0, and c parameter calculated as a function of β to impose a slope equal to Po at the middle of the Pc curve (Sw*=0.5).

The Kr simulation parameters detailed in Table 3 were taken, in addition to the Pc parameters for case 1 from Table 2 (Brooks-Corey Pc) and Pc parameters for case 2 and 3 indicated in Table 5.

Table 5. Simulation parameters for Pc

| CASE 1, Brooks-Corey Pc parameters		
Pce	0.52	psi
λ	0.476	
Iw	1,0	
CASE 2, log(beta) Pc parameters		
Po	11.6	psi
β	5	
Sw(Pc=0)	0,50	frac.
Iw	0,5	
CASE 2, log(beta) Pc parameters		
Po	11.6	psi
β	5	
Sw(Pc=0)	0,16	frac.
Iw	0,0	

The resulting Pc curves are shown in Figure 12 below:
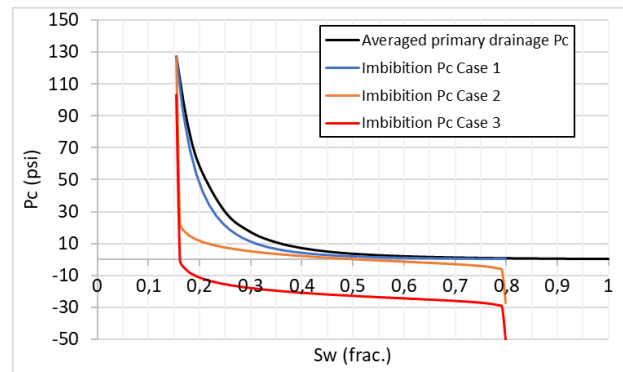
Fig. 12. Primary drainage (black) and imbibition capillary pressure curves for case 1 (blue), case 2 (orange) and case 3 (red)

The results from the three simulations are presented in Figure 13.
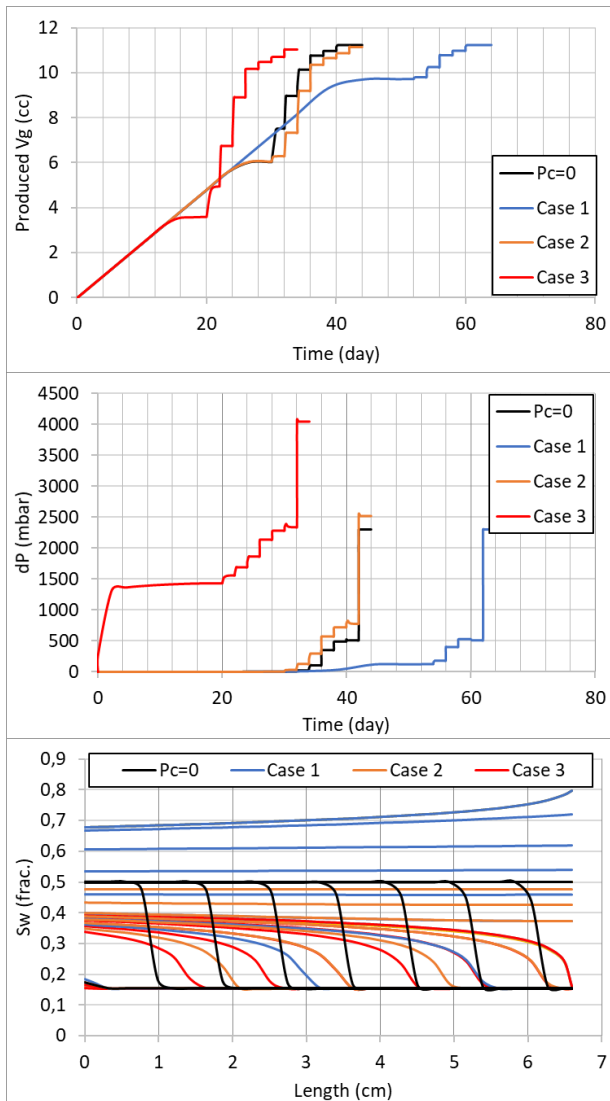
Fig. 13. Gas production, dP signal and saturation profiles during the first ratio (Qw=0.01cc/h – Qg=99.99cc/h)

The results from the simulations show that:

- The Pc effect is visible on the extreme cases in term of experimental durations, with shorter experiment with the least water-wetness condition and longer experiment with strongly water-wet condition

- More water-wet condition, longer and higher gas production at the first rate, but also lowest level of dP making the experiment almost not useable and uncertain, confirming that the steady-state Kr curve cannot be described over the full saturation range

- Case 2 and case with Pc=0 are very close regarding dP and produced Vg. Even with Iw=0.5, case 2 Pc curve remains flat, close to Pc=0 over a large range of saturation. Nevertheless, the saturation profiles are different (case 2 profiles tilted compared to "front like displacement" profiles at Pc=0)

- Case 3 results in short experimental duration, with readable high dP value and less produced Vg at the first ratio, allowing to potentially design an acceptable test. But the non-water wet Pc curve is not consistent with the measured Kr curve on the specific presented experiment. But it shows that, if the rock is not strongly water-wet compared to gas (as observed in the literature on some CO_2-brine coreflooding studies), it may be possible to measure the relative permeability curve

As explained in the last bullet point, imbibition gas-water Kr could be measured. But additional limitations can be encountered. As steady-state approach requires dP and produced Vg stabilization to calculate the relative permeability point at equilibrium, a lot of PVs must be injected through the sample: it may lead to some gas diffusion in water. Moreover, at high measured dP, gas compressibility and expansion may affect the in-situ saturation at ambient conditions: it is then preferable to perform more complex experiments at high pore pressure, with live fluids and specific HPHT separators and so on. Again, it only makes sense if the rock is not strongly water-wet.

6 Conclusions and Recommendations

In addition to a bibliography review on gas-water relative permeability and trapping relationship, experimental results from a consolidated sandstone reservoir study were compared with an indirect method to determine imbibition relative permeability. It is concluded that, after properly defining rock types using the measured primary drainage capillary pressure, the Brooks-Corey approach coupled with Land's hysteresis model is a good proxy for providing both drainage and imbibition gas-water relative permeability when water is strongly wetting the rock compared to gas. Due to the strong water wettability to the rock, it is extremely difficult or even impossible to experimentally determine imbibition relative permeability with unsteady-steady or steady-state coreflooding tests. The key parameters for the imbibition cycles are Krw Max and the Sgr-Sgi relationship: the shape of the Kr curve has negligible influence on the microscopic efficiency in imbibition cycle at strongly water-wet conditions, with very favorable viscosity ratio resulting in piston like displacement (no mobile gas behind the front).

It is not required to perform steady-state experimental test to attempt obtaining the imbibition gas-water Kr curve on water-wet rock. Numerical simulations confirmed this statement using the presented experimental case. Now, considering a non-water-wet system, as observed in some CO_2-brine studies at HPHT conditions, unsteady or steady-state coreflooding tests may be performed to capture the relative permeability curves.

All these observations confirm the findings in [6]: they will help in defining experimental protocols and interpretation of petrophysical parameters Kr and Pc in gas reservoirs with aquifer encroachment but also in saline aquifers that are identified as suitable storage formations for carbon dioxide (CO_2): in this last example, as the CO_2 plume rises upward in the formation due to the density contrast, the re-imbibition of water in the CO_2 flooded area will trap CO_2 as discontinuous non-wetting

phase: assessing the capacity of the aquifer to trap the CO_2 is obviously of high importance.

Nomenclature

C: Land's coefficient
CT: computed tomography
D: diameter, cm
dP: differential pressure, mBar
FTB: Fontainebleau outcrops
K: permeability, mD
Kg: gas permeability, mD
Kkl: Klinkenberg gas permeability, mD
Kw: water permeability, mD
Kw Max: maximum water permeability, mD
Kr: relative permeability
Krg: gas relative permeability
Krg Max: maximum gas relative permeability
Krw: water relative permeability
Krw Max: maximum water relative permeability
L: length, cm
MB: material balance
MICP: mercury injection capillary pressure
Ng: gas Corey exponent
Nw: water Corey exponent
Pc: capillary pressure
Pce: entry capillary pressure
p.u.: porosity unit
Qg: gas flow rate
Qw: water flow rate
Sg: gas saturation

Sg*: normalized/reduced gas saturation
SgF*: free and normalized/reduced water gas saturation
Sgi: initial gas saturation
Sgi*: normalized/reduced initial gas saturation
Sgr: residual gas saturation
Sgr*: normalized/reduced residual gas saturation
Sgrw: residual gas saturation post waterflood
Sgrm: maximum residual gas saturation with Sgi=1
Sw: water saturation
Sw*: normalized/reduced water saturation
Swi: irreducible water saturation
s.u.: saturation unit
Vg: produced gas volume

ε: function of λ, with ε=(2+3λ)/λ
φ: porosity
λ: pore size distribution index
ρg: gas density
μg: gas viscosity
ρw: water density
μw: water viscosity

References

1. Kumar, M. et al.: "Imaging of pore scale distribution of fluids and wettability", SCA 2008-16.

2. Lenormand, R. et al.: "Mechanisms of the Displacement of One Fluid by Another in a Network of Capillary Ducts", (1983), J. Fluid Mech., 135, 337-353.

3. Wardlaw, N.C.: "Fluid topology, pore size and aspect ratio during imbibition", Transport in Porous Media, 1988, V3,17-37.

4. Jerauld, G. et al.: "The effect of pore-structure on hysteresis in relative permeability and capillary pressure: Pore-level modeling", Transport in Porous Media, vol. 5, no. 2, pp. 103-151, 1990.

5. Blunt, M. et al.: "Pore-level modeling of wetting", Physical Review E, vol. 52, no. 6, pp. 6387- 6403, 1995.

6. Cense, A. et al.: "SCAL for gas reservoirs: a contribution for better experiments", SCA 2016-023.

7. Geffen, T. et al.: "Efficiency of gas displacement from porous media by liquid flooding", Transactions AIME, vol 195, 1952, p 29-38.

8. Legatski, M. et al.: "Displacement of gas from porous media by water", SPE 899, 1964.

9. Bull, O. et al.: "The quest for the true residual gas saturation- An experimental Approach", SCA 2011-03.

10. Pickell, J. et al.: "Application of air-Mercury and oil-air capillary pressure data in the study of pore structure and fluid distribution", SPEJ, March 1966, p 55-61, also SPE 1227.

11. MacKay, B.: "Laboratory studies of gas displacement from sandstone reservoir having strong water drive", APEA Journal 1974.

12. Handy, L.: "Determination of effective capillary pressure for porous media from imbibition data", Petroleum Transactions AIME, 1960, vol 219, p 75-80.

13. Chierici, G. et al.: "Experimental research of gas saturation behind the waterfront in gas reservoirs subjected to water drive", World Petroleum congress Frankfort, 19-26 June 1963.

14. Delclaud, J.: "Laboratory measurements of the residual gas saturation", SCA 1991-23 EURO, 1991.

15. Keelan, D.: "A critical review of core analysis techniques", JCPT, April-June 1972, p 42-55.

16. Fahes, M. et al.: "Wettability alteration to intermediate gas-wetting in gas-condensate reservoirs at high temperatures", SPEJ, December 2007, p 397-407.

17. Land, C. S.: "Calculation of Imbibition Relative Permeability for Two- and Three-Phase Flow from Rock Properties", SPEJ, (June 1968), 149.

18. Keelan, D.K. et al. : "Trapped-gas saturation in carbonate formations", SPE 4535, (1975).

19. Aissaoui, A.: "Etude théorique et expérimentale de l'hystérésis des pressions capillaires et des perméabilités relatives en vue du stockage souterrain de gaz", PhD thesis, Ecole des Mines de Paris, 1983.

20. Jerauld, G.: "General three phase relative permeability model for Prudhoe Bay", SPERE 12(4) p 255-263, 1997

21. Suzanne, K. et al.: "Residual gas saturation of sample originally at residual water saturation in heterogeneous sandstone reservoirs", SCA 2003-14.

22. Suzanne, K. et al.: "Distribution of trapped gas saturation in heterogeneous sandstone reservoirs", SCA 2001-14.

23. Hamon, G. et al.: "Field-wide variations of trapped gas saturation in heterogeneous sandstone reservoirs", SPE 71524, 2001.

24. Suzanne, K. et al.: "Experimental relationships between residual gas saturation in heterogeneous sandstone reservoirs", SPE 84038, 2003.

25. Purcell, W. R.: "Capillary Pressures – Their Measurement Using Mercury and the Calculation of Permeability" Trans. *AIM*E, (1949), 186, 39.

26. Burdine, N. T.: "Relative Permeability Calculations from Pore Size Distribution Data" *Trans. AIME*, (1953), 198, 71.

27. Corey, A. T.: "The Interrelation between Gas and Oil Relative Permeabilities", Prod. Mon. (1954), 19, 38.

28. Brooks, R. H. and Corey, A. T.: "Properties of Porous Media Affecting Fluid Flow", *J. Irrig. Drain. Div.*, (1966), 6, 61.

29. Leverett, M.C.: "Capillary behavior in porous solids". *Transactions of the AIME* (142): 159–172, 1941.